ITM Web of Conferences **84**, 04019 (2026) https://doi.org/10.1051/itmconf/20268404019
ATCIDS 2026

Validation of The Scale Model of The Semi-automatic Lifebuoy Throwing Robot

Bo Gao[*], *Yuan* Dong, *Chengcheng* Yang, *Shiyao* Zhang and *Yuyi* Zou

School of Mechanical and Electronic Control Engineering, Beijing Jiaotong University, Beijing, China, 100044

Abstract. China's extensive coastlines, inland rivers, and numerous reservoirs present persistent risks of drowning accidents, highlighting a critical need for technological intervention in water safety and emergency response. To address the urgent challenge of reducing response time and improving rescue success rates, this paper focuses on the research and development of an automated rescue device. Specifically, we present the design, implementation, and evaluation of a novel semi-automatic lifebuoy-launching robot. The development process involved a systematic analysis of operational requirements, leading to the creation of a compact, modular mechanical structure optimized for stability and rapid deployment. The core electronic control system integrates machine vision for initial target detection, a precise motor-driven launching mechanism, and a reliable wireless communication module for remote operator control. This combination allows for a "human-in-the-loop" operation where an operator confirms the target and triggers the launch, ensuring decision-making reliability. A series of controlled experiments and field tests were conducted in simulated environments, including swimming pools and calm open-water areas. The results demonstrate that the robot can consistently and accurately project a standard lifebuoy to a designated target zone within a defined range, effectively bridging the critical gap before human rescuers arrive. The system proves to be a practical and efficient technological aid, capable of enhancing the existing rescue framework. This study not only validates a functional prototype but also provides a significant reference point for the future development of more autonomous, intelligent, and adaptive robotic systems in aquatic rescue, potentially contributing to a substantial decrease in water-related fatalities.

1. Introduction

China's water area is approximately 270,550 square kilometers, which is very vast. While it boasts beautiful scenery and abundant resources, the extensive water area also leads to some personal safety problems. In rivers, lakes, or coastal areas, people can often be seen swimming and playing in the water, and there are also frequent water activities in enclosed

[*] Corresponding author's email: gaobo1@bjtu.edu.cn

indoor environments such as water parks. Whether indoors or outdoors, drowning accidents have always been one of the biggest potential safety hazards in water recreational activities. According to statistics from the National Health Commission, about 59,000 people die from drowning in China every year, among which minors account for more than 95% [1]. When a drowning accident occurs, the timeliness of rescue often determines the life or death of the drowning person. However, if rescuers without professional life-saving skills blindly enter the water to save people, it is likely to cause a vicious accident of "one person falling into the water and multiple people dying". Therefore, it is particularly important to develop water rescue equipment to ensure the life safety of drowning people, avoid rescuers falling into danger, and thus improve the success rate of rescue.

At present, some common large-scale water rescue robots have comprehensive functions, but they are bulky and not easy to store. Meanwhile, they are complex to operate, requiring transportation by large mechanical equipment and auxiliary operation by professional personnel. The equipment maintenance cost is high, and they are usually not suitable for urban inland river environments and indoor water entertainment venues [2]. In view of the above situation, this paper designs a precise
lifebuoy launching robot with small size, strong power, complete functions, stable performance, and capable of rapid rescue, and verifies the scale model of the robot (hereinafter referred to as the robot).

The function of the robot in this paper is to throw lifebuoys, which can launch lifebuoys to drowning people, thereby avoiding drowning accidents to a certain extent. To meet the above expectations, the robot is required to be able to skillfully pick up and launch lifebuoys, as well as move freely on the site. For the convenience of model verification, the lifebuoy is simplified into a circular ring in this paper. Two robots are designed from the aspects of mechanical structure and control system. Effective and reasonable control is carried out on the basis of optimizing the structure, and the stable and reliable realization of the robot's functions is ensured on the premise of safety. Overall design drawing of the robot is shown in figure 1.

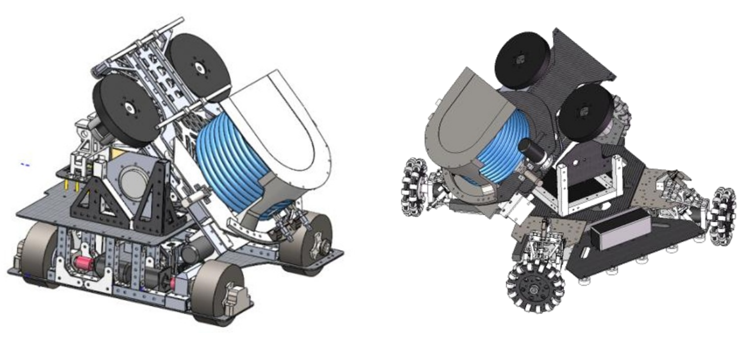

Fig 1. Overall design drawing of the robot

2. Mechanical Structure Design

2.1 Robot Chassis Design

To complete the tasks of point-to-point movement at a relatively high speed and picking up circular rings, while taking into account safety, stability, and flexibility, the robot chassis is designed rigorously in this paper.

The chassis of Robot 1 (as shown in Figure 2) adopts a two-layer aluminum alloy structure, which has the characteristics of low weight, high rigidity, and high precision. The chassis uses four omnidirectional wheels distributed in a cross shape as executive wheels, and can achieve movement in any direction by controlling the differential speed of the omnidirectional wheels [3]. To ensure the stability of the chassis and the accuracy of the launching mechanism, each of the four omnidirectional wheels of Robot 1 is equipped with an independent suspension mechanism, which ensures that all omnidirectional wheels are in contact with the ground at the same time, avoiding shaking caused by the four wheels not being on the same plane.

The chassis structure design of Robot 2 is shown in Figure 2. The chassis adopts a two-layer carbon plate structure, which is lighter in weight while ensuring sufficient strength and rigidity. Its chassis uses four Mecanum wheels as executive wheels, and can realize omni-directional movement and lateral movement of the vehicle body on the horizontal plane by controlling the steering of the four Mecanum wheels.

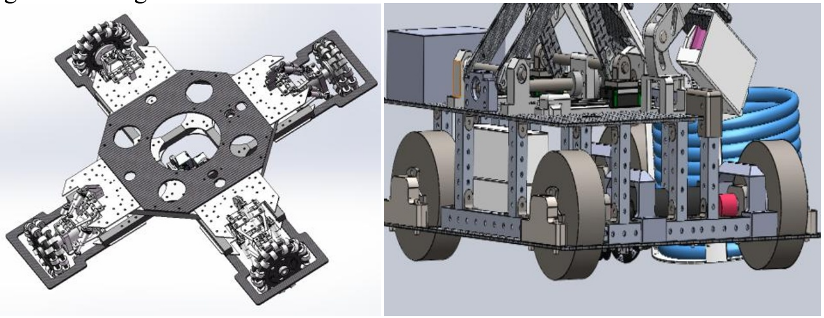

Fig 2. Chassis design drawings of Robot 1 and Robot 2

2.2 Picking Mechanism Design

The picking mechanisms of the two robots have the same principle. By consulting databases such as CNKI, VIP, and Wanfang, it is found that the research on the picking mechanisms of rescue robots in China mainly focuses on the design and development of manipulators. Based on the research status, this paper adopts a scheme of pneumatic grasping combined with a mechanical arm.

After practical verification, the scheme has the following problems:

After grasping the circular ring, it is necessary to complete the flipping action at the same time. The movement range of the gripper and rocker arm relative to the chassis is large. When the gripper flips, the center of gravity of the mechanism is unstable, the stability is poor, and the load-bearing capacity is small.

The initially designed gripper and mechanical arm have many kinematic pairs, and the control part is relatively complex.

The gripper can only grasp one circular ring at a time, resulting in low efficiency.

Based on the above problems, the picking mechanism is redesigned. As shown in Figure 3, the new mechanism adopts the idea of shoveling to obtain circular rings. When picking up the ring, the mechanism flips to a specified position, and the shovel-shaped structure composed of arc-shaped iron sheets and upper limiters can pick up multiple circular rings at the same time and flip back to reset. The mechanism only needs one kinematic pair, and has the characteristics of higher stability, higher efficiency, and larger load-bearing capacity. The actual test shows that the single loading only takes 4.8 seconds, which initially meets the design expectations.

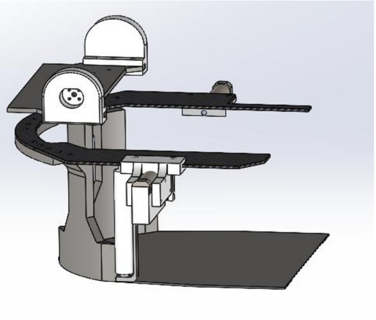

Fig 3. Design drawing of the picking mechanism

2.3 Launching Mechanism Design

The launching mechanism is the core component of the robot's mechanical structure, and its function is to provide appropriate power for the circular ring so that it can fly out at a certain speed and direction. The two robots adopt similar launching mechanisms, which are mainly composed of three parts: the ring launching mechanism, the pitching mechanism, and the rotating mechanism.

2.3.1 Ring Launching Mechanism

This paper designs a ring launching mechanism based on N5065 brushless motor, M3508 brushless motor, and friction wheel, whose structure is shown in Figure 4. Distribution diagram of landing points is shown in figure 5.

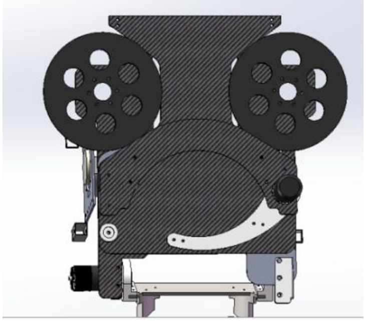

Fig 4. Design drawing of the launching mechanism

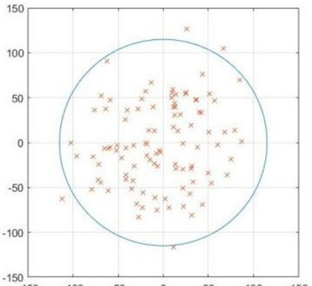

Fig 5. Distribution diagram of landing points

The working principle of the launching mechanism is as follows: the paddle rotates to give the circular ring an initial speed, and then the friction wheel contacts the circular ring to transmit power to the circular ring, so that the circular ring is shot out at a certain speed. By controlling the speed of the N5065 brushless motor, the launching speed and distance of the circular ring can be adjusted. The actual test shows that the maximum linear launching speed of the circular ring can reach 28.8 m/s, and the maximum launching distance can reach 12 m. The design of the ring launching mechanism fully considers factors such as the size, weight, shape, and material of the circular ring to ensure that the circular ring can be launched stably, thereby ensuring the accuracy of launching. After many repeated experiments, the distribution of the landing points of the circular ring is obtained as shown in Figure 5. For a single fixed point, the hit rate of the circular ring is about 96%, which has a high hit rate, proving that the robot design is effective and feasible.

2.3.2 Pitching Mechanism

To realize the launching of the circular ring at any angle, it is necessary to adjust its launching angle to adapt to targets of different heights. This paper designs a pitching mechanism based on a permanent magnet synchronous motor to adjust the launching angle of the circular ring. Figure 6 is a schematic diagram of the pitching mechanism.

The pitching mechanism has a simple structure, is not easy to fail, and has a large adjustment range of -30° to 70°. Its frame is composed of lightweight materials such as resin plates, carbon plates, and carbon tubes to reduce self-weight and inertia, and improve the stability and accuracy of the mechanism. The mechanism uses a GO-M8010-6 permanent magnet synchronous motor as the power source, controls the torque of the motor through an electronic speed controller, and performs closed-loop control on the angular position of the motor, thereby realizing fast and precise angle control.

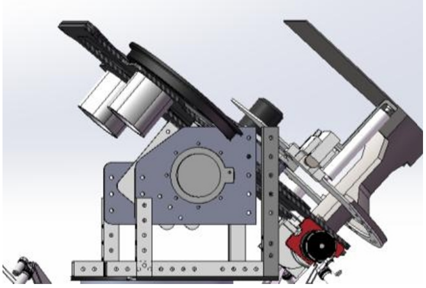

Fig 6. Design drawing of the pitching mechanism

2.3.3 Rotating Mechanism

To realize the function of launching circular rings in different directions at a fixed point, this paper designs a rotating mechanism based on an internal meshing gear pair, M3508 brushless motor, and dining table bearing. The adjustment range of the mechanism is 360°, and it performs closed-loop reverse control through an absolute value rotary encoder, which has the advantages of strong load-bearing capacity, fast speed, and high precision.

3. Design of the Control Part

3.1 Hardware Selection

To achieve the function of projecting rubber rings and meet the requirements of high robustness and accuracy, this paper builds a control system based on the RoboMaster Development Board Type A main controller, selects DJI M3508 motor as the main motor for movement, and uses the Action positioning module to provide precise position.

3.1.1 Main Controller Board

The RoboMaster Development Board Type A is a high-performance control board based on the STM32F427IIH6 chip, with a working frequency of up to 180 MHz. The STM32F427 device includes high-speed embedded memory, up to 4 kb of backup SRAM, and a variety of peripherals and interfaces, which meet the application needs of this robot.

At the same time, this type of development board also has the characteristics of small size, light weight, and perfect insulation protection and reverse connection prevention measures. Therefore, this ring-launching robot is developed based on it, giving full play to the precise control of the ring's flying attitude and speed as envisaged by the mechanism.

3.1.2 M3508 DC Brushless Gear Motor

The M3508 DC brushless gear motor has strong versatility and is used in the chassis, ring picking and other mechanisms of this robot. The motor can perform torque control, with both high torque and speed. The reduction ratio of the gearbox is about 19:1 [4], which is suitable for high-speed and heavy-load scenarios. The motor communicates with the main controller through the CAN bus, has a high control frequency and a variety of configurable ID numbers, and is also suitable for large-scale use in robot systems. At the same time, the price of the motor is relatively reasonable, reducing the cost of this robot.

3.1.3 ACTION Full-Field Positioning Module

This positioning system integrates various sensors such as IMU and magnetic encoder for buyers to use. Through the fusion of its sensor data and Kalman filtering, more accurate pose information of the center of the positioning system in the world coordinate system can be obtained. The suspension design of the orthogonal omnidirectional wheels also greatly improves the accuracy of the odometer and the grip of the module. The rated 5V power supply of this module can be directly provided by the main controller board, and data can be configured and output through the RS232 serial port module. This robot uses an RS232 to TTL serial port level conversion module to directly connect it to the main board for serial communication to read the robot's pose information.

3.2 Motion Algorithm Design

The design of the motion algorithm mainly includes two aspects: the basic control algorithm and the chassis motion model. Finally, various tasks are coordinated and realized through the uC-OSIII operating system. The control algorithm controls the motion chassis through the incremental PID algorithm to realize two motion strategies: the speed loop and the position loop, so as to achieve stable speed and accurate position. The motion model is an algorithm for the movement of the chassis. It can inversely calculate the desired speed or desired position of the robot in the world coordinate system to the speed of each motor of the chassis through the upper-layer main control code.

3.2.1 Motion Model

This robot adopts two types of wheels: Mecanum wheels and omnidirectional wheels, so it is necessary to establish different motion models for them respectively. Assume that the robot needs to complete rotation and horizontal translation at the same time. The robot can be defined as follows:

V_x is the component speed in the x direction.

V_y is the component speed in the y direction.

ω is the rotational angular velocity.

Then we have:

$$V_x = V_{tx} - \omega r \tag{1}$$

$$V_y = V_{ty} + \omega r \tag{2}$$

(1) Mecanum Wheel Motion Model

Mecanum wheels have 45° freely rotating rollers and are divided into two types: A and B [5]. Therefore, the linear speed of Mecanum wheels is in the 45° direction, and the X-type installation mode is adopted in this paper.

Based on the above formula, the following model is obtained, where $V_{\omega i}$ is the linear speed of the i-th wheel. Taking the upper left wheel as wheel 1, rotating counterclockwise for a week, the other wheels are numbered 2, 3, and 4 in turn. The half-length of the robot in the x direction is a, and the half-length in the y direction is b.

The model is as follows:

$$V_{\omega 1} = V_{ty} - V_{tx} + (a + b)\omega \tag{3}$$

$$V_{\omega 2} = V_{ty} + V_{tx} - (a + b)\omega \tag{4}$$

$$V_{\omega 3} = V_{ty} - V_{tx} - (a + b)\omega \tag{5}$$

$$V_{\omega 4} = V_{ty} + V_{tx} + (a + b)\omega \tag{6}$$

(2) Omnidirectional Wheel Motion Model

Omnidirectional wheels have free rollers on the wheel circumference, so the omnidirectional wheels are installed at 90° to each other. Therefore, the wheels can not only rotate tangentially but also axially. Similarly to the Mecanum wheel motion model, the following model is obtained:

$$V_{\omega 1} = \sqrt{2}V_{ty} - \sqrt{2}V_{tx} + (a + b)\omega \tag{7}$$

$$V_{\omega 2} = \sqrt{2}V_{ty} + \sqrt{2}V_{tx} - (a + b)\omega \tag{8}$$

$$V_{\omega 3} = \sqrt{2}V_{ty} - \sqrt{2}V_{tx} - (a + b)\omega \tag{9}$$

$$V_{\omega 4} = \sqrt{2}V_{ty} + \sqrt{2}V_{tx} + (a + b)\omega \tag{10}$$

3.2.2 PID Algorithm

The control formula of the PID algorithm is:

$$u(t) = K_p\left[e(t) + \frac{1}{T_i}\int_0^t e(\tau)d\tau + T_d\frac{de(t)}{dt}\right] \tag{11}$$

Where:

$u(t)$ is the control quantity output by the controller;

$e(t)$ is the error signal, which is equal to the difference between the given quantity and the output quantity;

K_p is the proportional coefficient (P), T_i is the integral time constant (I), and T_d is the differential time constant (D) [6].

In the design of the PID algorithm this time, the incremental PID is selected, that is, the error $e(t)$ in the transfer function is obtained by subtracting the previous error from the current error, and $\frac{de(t)}{dt}$ is equal to $e(k) - 2e(k-1) + e(k-2)$, that is, current error - 2previous error + the error before the previous one. Once K_p, T_i, and T_d are determined, the control increment can be calculated by the formula only with the deviations of the previous three measured values. The obtained control quantity is the increment of the position errors in recent times, not the deviation corresponding to the actual position, which means there is no error accumulation. Therefore, a good control effect is easy to obtain through weighted processing, and when there is a problem with the system, the incremental PID will not seriously affect the operation of the system [7]. The PID designed this time is set as a triple PID nested structure: position loop PID, speed loop PID, and angular velocity PID.

Angular Velocity PID: During the movement, it is necessary to decompose the total desired speed into the linear speed of each wheel and convert it into the speed of the motor according to the parameters of the wheel. To ensure that the angular velocity remains constant under any conditions, it is necessary to introduce the angular velocity PID [8]. The desired value is the angular velocity sent by the main controller to the driver through CAN communication, and the actual value is the angular velocity measured in real-time by the encoder. The adjustment of PID is completed inside the driver, independent of the main controller, and the PID parameters are directly written by connecting the driver through the upper computer.

Speed Loop PID: The function of this PID is to compare and correct the desired speed with the actual speed. The actual speed is obtained by the Action positioning module mentioned above, and the goal is to make the robot stably reach the set speed and maintain it.

Position Loop PID: The desired speed is determined by the current distance to the end point, which should roughly follow an acceleration-constant speed-deceleration process with the distance. However, giving the desired speed according to the actual distance may lead to overshooting the end point even if the speed decreases before the end point, and then oscillate back and forth [9]. Through the position loop PID, the distance for solving the desired speed and the actual distance are adjusted according to the actual distance under different actual distance conditions.

The algorithm designed this time starts from the position fed back by the input positioning module and the desired position of the traveling route, and outputs a specific desired speed for the rotation of the steering wheel motor through the nested three-layer PID algorithm from the sensor feedback to the control chip and then to the motion mechanism, which greatly improves the control accuracy of the robot.

3.2.3 Kalman Algorithm

The prediction equations are:

$$x_k^- = Ax_{k-1} + Bu_{k-1} \tag{12}$$

$$P_k^- = AP_{k-1}A^T + Q \tag{13}$$

The correction equations are:

$$K_k = \frac{P_k^- H^T}{HP_k^- H^T + R} \tag{14}$$

$$x_k = x_k^- + K_k(z_k - Hx_k^-) \tag{15}$$

$$P_k = (I - K_k H)P_k^- \tag{16}$$

This method is based on state space prediction. By formulating state space equations, it first predicts and then corrects. This robot locates the robot through three-dimensional Kalman filtering from acceleration to speed and then to position. To solve the cumulative error caused by the long-term operation of the system, this paper uses the state error Kalman filtering algorithm. In the position estimation using Kalman filter, a large part does not directly take the system position as the state of the Kalman filter, but takes the integral error of position and the error of speed as the system state. The output of speed is compensated for the estimated speed error, and then integrated to obtain the estimated attitude angle, which is then compensated for the estimated attitude angle error.

In this paper, the position observation value is obtained by the ACTION full-field positioning module, the speed observation value is obtained by differentiating with the laser sensor, and finally, the acceleration information is obtained by the on-board IMU by preheating the heating resistor to control temperature drift. The error value is used as input, and Kalman filtering is performed to obtain the following positioning experimental results:

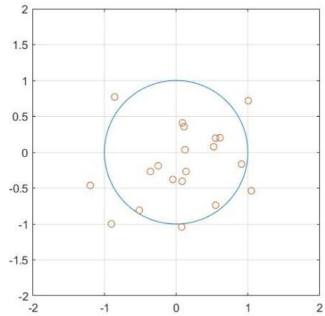

Fig 7. Laser positioning deviation diagram

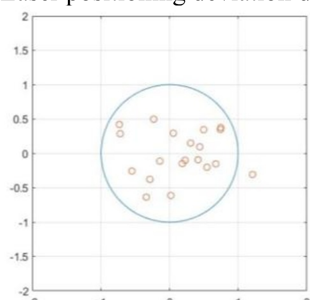

Fig 8. Traditional Kalman filter positioning deviation diagram

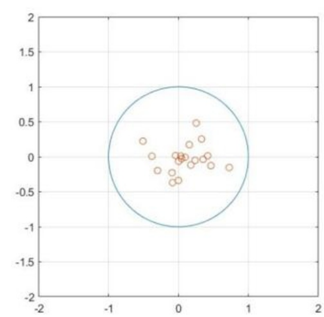

Fig 9. State error Kalman filter positioning deviation diagram

It can be seen from figure 7, figure 8 and figure 9 that after using the state error Kalman filter, the variance of positioning is significantly reduced, and the positioning accuracy and stability are greatly improved.

4. Conclusion

This paper presents the design and validation of a semi-automatic lifebuoy-throwing robot using an STM32F427 MCU as the main controller. Through systematic analysis and innovation in the overall mechanical structure, along with optimization and testing of motion control algorithms, the scale model of the robot has been successfully verified, achieving semi-autonomous operation in simulated rescue scenarios. The feasibility of the system is supported by experimental results: the robot achieves a high hit rate (approximately 96%) within a range of up to 12 meters, with a maximum launch speed of 28.8 m/s. Its omnidirectional mobility, reliable ring-picking mechanism, and human-in-the-loop control mode offer a practical and efficient aid for initial water rescue, potentially reducing response time before professional assistance arrives. However, several limitations remain: the current prototype has only been tested in calm water conditions, with performance in waves, currents, or adverse weather yet to be evaluated; the lifebuoy is simplified as a uniform ring, differing from real buoys in size, weight, and buoyancy; the system relies on external positioning and wireless communication, which may be susceptible to real-world interference; and energy autonomy, durability in aquatic environments, and cost-effectiveness for widespread deployment require further investigation. Future work will focus on developing a full-scale prototype, enhancing environmental adaptability, improving target detection robustness, and advancing the level of autonomy, with the goal of implementing the system in practical water rescue operations.

Acknowledgement

The first two authors, Bo Gao and Yuan Dong, contributed equally to this work.

References

1 Dai Mengna, Xi Yan, Yin Wenqiang, et al. Current status and trend analysis of drowning deaths among children aged 0-14 in China from 1990 to 2019 [J]. Chinese Journal of School Health, 2022; 256-259.

2 Sheng Xiaowei, Yu Linxin. Design of a small intelligent water rescue robot [J]. Jiangsu Vocational Institute of Engineering and Technology, 2022.

3 Zhang Sen. Design and motion control research of all-wheel steering mobile chassis [D]. Xi'an University of Technology, 2021.

4 Yang Haijun, Hou Yongqi, Wang Lixiang, Cao Yunlong, Jiao Hongtao, Yang Hao. Design of a Bluetooth positioning express delivery robot based on ROS [J]. Technology Innovation and Application, 2021, 11(27): 65-69+72.

5 Xu Meng. Research on positioning algorithm and experiment of mobile chassis of transfer robot [D]. Beijing Institute of Petrochemical Technology, 2021.

6 ZHOU L, HU Q, PENG X, et al. Real-Time Proportional-Integral-Derivative (PID) Tuning Based on Back Propagation (BP) Neural Network for Intelligent Vehicle Motion Control[J]. Computers, Materials and Continua, 2025,83(2): 2375-2401.

7 ZHOU L, HU Q, PENG X, et al. Real-Time Proportional-Integral-Derivative (PID) Tuning Based on Back Propagation (BP) Neural Network for Intelligent Vehicle Motion Control[J]. Computers, Materials and Continua, 2025,83(2): 2375-2401.
8 CHEN K, ZHOU H, SHAN X. Rotation-control device for construction cranes with nested PID control[J]. Automation in Construction, 2023,146: 104704.
9 ZHANG Y, YANG T, LI C, et al. Fuzzy-PID control for the position loop of aerial inertially stabilized platform[J]. Aerospace Science and Technology, 2014,36: 21-26.
10 Li Gelun. Design of motion control system for wheeled mobile robots. Northeast Agricultural University, 2018.